SPIN INTERACTIONS AT THE INTERFACES FERROMAGNETIC OXIDE/FERROMAGNETIC INTERMETALLIC SUPERLATTICE

Alexey Klimov, Viktor Demidov, Timur Shaykhulov, Gennady Ovsyannikov, Karen Constantinian, Sergey Nikitov, Vladimir Preobrazhensky, Nicolas Tiercelin, Philippe Pernod

SPIN INTERACTIONS AT THE INTERFACES FERROMAGNETIC OXIDE/FERROMAGNETIC INTERMETALLIC SUPERLATTICE

Alexey A. Klimov
MIREA- Russian Technological University, http://mirea.ru
Moscow 119454, Russian Federation

Viktor V. Demidov, Timur A. Shaykhulov, Gennady A. Ovsyannikov, Karen Y. Constantinian, Sergey A. Nikitov
Kotelnikov Institute of Radioengineering and Electronics of RAS, http://cplire.ru/
Moscow 125009, Russian Federation

Vladimir L. Preobrazhensky
Prokhorov General Physics Institute of RAS, http://igp.ras.ru/
Moscow 119991, Russian Federation

Nicolas Tiercelin, Philippe Pernod
Institut d'Electronique, de Microélectronique et de Nanotechnologie, Université de Lille, https://www.iemn.fr/
Centrale Lille, ISEN, Univ Valencienes UMR 8520-IEMN, LIA LICS/LEMAC, F- 59652, Villeneuve d'Ascq Cedex, France

aleks-klimov@yandex.ru, demidov@cplire.ru, shaihulov@hitech.cplire.ru, gena@hitech.cplire.ru, karen@hitech.cplire.ru, vladimir.preobrajenski@univ-lille.fr, nicolas.tiercelin@univ-lille.fr, philippe.pernod@univ-lille.fr, nikitov@cplire.ru

Abstract. **The magnetic properties of the heterostructures consisting of platinum Pt, epitaxially grown manganite optimally doped by strontium $La_{0.7}Sr_{0.3}MnO_3$ (LSMO), rare earth intermetallic superlattices consisting of exchange-coupled layers $TbCo_2$/FeCo (TCFC), and the epitaxial film of yttrium iron garnet $Y_3Fe_5O1_2$ (YIG) were investigated. The TCFC material provides giant magnetostriction, large magnitude of the magnetomechanical coupling coefficient, and controlled induced magnetic anisotropy. In addition TCFC, as well as Pt, has strong spin-orbit interaction. Experimental studies have shown that the magnetic interaction of the heterostructure ($TeCo_2$/FeCo)n/LSMO has an antiferromagnetic character. An increase of linewidth of the ferromagnetic resonance in the Pt/LSMO structure was observed and explained by the spin current flow induced in Pt film by the LSMO film at ferromagnetic resonance. In the TCFC/YIG heterostructure, an electric voltage induced in the TCFC film was observed and explained by the inverse spin-Hall effect under conditions of ferromagnetic resonance.**

Keywords: **heterostructure, manganite, intermetallic superlattice, yttrium iron garnet, ferromagnetic resonance, spin current, inverse spin-Hall effect**

PACS: 75.47.Lx, 75.25.-j, 75.70.Cn, 71.20.Lp

Bibliography - 34 references *Received 12 November 2018; accepted 10 December 2018*

RENSIT, 2018, 10(3):363-372 **DOI: 10.17725/rensit.2018.10.363**

Contents

1. INTRODUCTION

The development of spintronic devices based on magnetoactive materials with the nanoscale interfaces is an important task, which requires the study of the physics of structural and phase transformations in thin films and at the interfaces. Spintronics is based on phenomena associated with the transfer of the spin moment. A "pure" spin current can be created by several

mechanisms, among which the most effective are the spin-Hall effect [1] and the spin pumping in ferromagnetic resonance mode [2]. The magnetic heterostructure as a rule consists of magnetic and nonmagnetic layers. Materials with a strong spin-orbit interaction play an important role in the detection of the spin current. A pure spin current (J_S) can be detected using the inverse spin-Hall effect (ISHE) in a material with strong spin-orbit interaction by converting into conduction current $J_c = \theta_{SH}(\hbar/2e)(J_S \cdot \sigma)$, where θ_{SH} is the angle of spin-Hall effect, σ - carrier polarization.

However, not only non-magnetic normal metals can be used as ISHE spin current detectors. In a number of works, it was shown that magnetic metals, such as permalloy Py (NiFe), as well as Fe, Co, Ni can be used as spin current detectors [3-5]. $TbCo_2$/FeCo structures containing Tb element with a strong spin-orbit interaction (high atomic weight *Z*) are distinguished by giant magnetostriction, a large value of the magnetomechanical coupling coefficient, controlled induced magnetic anisotropy and the ability to induce spin-orientation transitions by a magnetic field or elastic stresses [6, 7]. In turn, rare earth manganite perovskites with the structure $Re_{1-x}A_xMnO_3$ (Re are rare earth materials such as La or Nd), and A - alkaline earth metals such as Sr, Ca, Ba) exhibit a wide range of unusual electrical and magnetic properties, including high (up to 100 %) magnetic polarization, the effect of colossal magnetoresistance, etc (see review [8]). Manganite films for which the Curie temperature T_C is close to room temperature is especially attractive for practical use. A number of studies on the excitation of the spin current by ferromagnetic resonance in LSMO/N structures (N is a normal metal, usually platinum) were made in [9, 10]. However, there are no data on the temperature dependences of the width of the ferromagnetic resonance (FMR) line during the generation of spin current in ferromagnets and on the magnitude of the spin conductivity of the LSMO/Pt boundary. We have investigated the magnetic properties of heterostructures consisting of platinum Pt, epitaxially grown manganite $La_{0.7}Sr_{0.3}MnO_3$ (LSMO), rare earth intermetallic superlattices consisting of exchange-coupled layers $TbCo_2$/FeCo (TCFC), and the epitaxial film of yttrium iron garnet $Y_3Fe_5O_{12}$ (YIG). Our studies are focused on the effects associated with the excitation and generation of spin current in the structures.

2.FERROMAGNETIC RESONANCE IN MANGANITE EPITAXIAL FILMS

The Hilbert damping parameter α is a measure of the spin precession relaxation in homogeneous ferromagnets caused by spin-orbit interaction [11]. The width of the homogeneous FMR line induced by Hilbert damping is proportional to the FMR frequency ω, $\Delta H_G = \alpha\omega/\gamma$ ($\gamma = g\mu_B/\hbar$ is the gyromagnetic ratio) and describes the situation for the homogeneous case. In the ferromagnetic structure of a ferromagnet and a normal metal, the FMR line is additionally broadened due to the generation of the spin current, inhomogeneity of the magnetization of the ferromagnet, interaction with another material, two-magnon scattering and the appearance of eddy current in the ferromagnet. As a result, the FMR linewidth can be represented as a sum

$$\Delta H_{PP} = \Delta H_G + \Delta H_I + \Delta H_{2M} + \Delta H_E, \quad (1)$$

where ΔH_I, ΔH_{2M}, ΔH_E are the widths of the lines for damping caused by the inhomogeneous state of a ferromagnet, two-magnon scattering and damping caused by eddy current, respectively [12, 13]. A change in the magnetic properties of materials such as its anisotropy or magnetization affects the inhomogeneous broadening of the FMR line (ΔH_I) which is independent of frequency [12, 13]. The magnetic field of an alternating current caused by FMR induces eddy currents in a thin conductive film. These currents produce an additional change in the amplitude of the alternating current magnetic fields of the heterostructure. The influence of eddy currents on ferromagnetic resonance in a conducting ferromagnetic system can lead to

broadening of the FMR linewidth (ΔH_E) and to the change in the shape of the FMR spectrum at non-uniform microwave field [14-16]. The mechanism of two-magnon scattering leads to the connection of homogeneous precession (k = 0) with degenerate finite spin-wave modes [17, 18]. In a ferromagnet/normal metal heterostructure the precession of magnetization in a ferromagnet causes a spin current to flow through the boundary into the normal metal, which broadens the FMR line. The theory [19] predicts the spin current to flow through the boundary of the ferromagnetic and nonmagnetic layers perpendicular to the interface.

The linewidth of ferromagnetic resonance ΔH_{pp}, measured by scanning the external magnetic field H, is defined as the difference in the field positions between the extremes H_{p+}, H_{p-} of the first derivative of the dP/dH microwave absorption signal (see **Fig. 1**). At this value, the resonance field H_0, defined as the point of transition of the signal dP/dH through zero is always in the range $H_{p+} < H_0 < H_{p-}$. Note, that the determination of the linewidth by approximating the FMR spectrum by several Lorentz lines gives an approximate 10% correction in the value of ΔH_{pp}.

Experimental studies were performed on $La_{0.7}Sr_{0.3}MnO_3$ (LSMO) epitaxial films, which were deposited by magnetron sputtering onto (110) $NdGaO_3$ (NGO) single crystal substrates at T = 820°C and oxygen pressure of 0.15-1 mbar. Pt films 10-20 nm thick were deposited ex situ immediately after cooling of the manganite film. Magnetic characteristics were measured by FMR using a Bruker spectrometer (frequency 9.51 GHz). The experimental samples were located in the microwave cavity of the spectrometer so that the sample plane was always parallel to the direction of the constant external magnetic field and the magnetic component of the microwave field (parallel orientation). The method of sample preparation and FMR measurements are described in [20]. Obtained films were investigated immediately after the deposition and cooling to room temperature (d-LSMO), and were annealed after the growth at T = 820°C for one hour (h-LSMO). For h-LSMO films, 40 nm thick, we determined the attenuation α_0 of the spin precession at room temperature from linewidth ΔH_{PP} = 28 Oe which corresponds to $\alpha_0 = \Delta H_{PP} \cdot \gamma/\omega = 8 \cdot 10^{-3}$. The increase in attenuation $\alpha = \alpha_0 + \alpha'$ during the deposition of Pt on the LSMO can occur due to the flow of the spin current through the Pt/LSMO boundary. For Pt deposited on the h-LSMO film with thickness of 10 nm the parameter α increases by 10%. Using [21, 22], one can calculate the spin conductivity in the Pt/LSMO heterostructure:

$$g^{\uparrow\downarrow} = \frac{4\pi M_s t_{LSMO}}{g\mu_B}\alpha', \qquad (2)$$

where $\gamma = 17.605 \cdot 10^6$ is gyromagnetic ratio for an electron, $\omega = 2\pi \cdot 9.51 \cdot 10^9 s^{-1}$ is microwave angular frequency, M_s = 300 Oe is LSMO film magnetization, t_{LSMO} = 40 nm is LSMO film thickness, $\mu_B = 9.274 \cdot 10^{-21}$ erg/G is the Bohr magneton, g = 2 is the Lande factor. At room temperature, an increase in the FMR linewidth after deposition of Pt $\Delta H_{Pt/LSMO} - \Delta H_{LSMO} = 4$ Oe and, therefore, $g^{\uparrow\downarrow} = 0.4 \cdot 10^{19}$ m^{-2} was obtained. This value of the spin conduction of the boundary slightly exceeds $g^{\uparrow\downarrow} \sim 10^{18}$ m^{-2}, obtained from measurements of the spin current on the same Pt/LSMO structures using the inverse spin-Hall effect [23]. For comparison, $g^{\uparrow\downarrow} = 2.1 \cdot 10^{19}$ m^{-2}

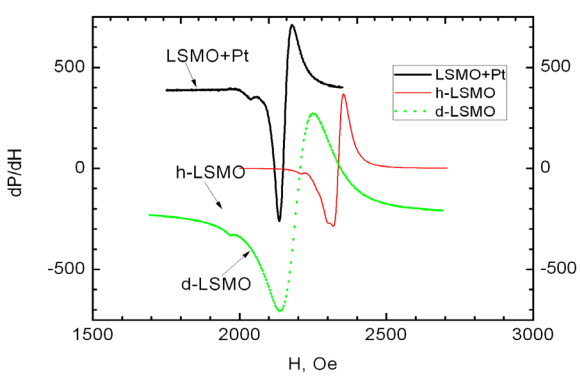

Fig. 1. *FMR spectra for d-LSMO and h-LSMO films and Pt/h-LSMO heterostructures. Spectra for d-LSMO and Pt/h-LSMO are shifted along the dP/dH axis.*

[24] was obtained for Py/Pt boundaries, and $g^{\uparrow\downarrow} = 4.8 \cdot 10^{20}$ m^{-2} [25] for YIG/Pt.

When estimating the spin conductivity, using (2), other mechanisms of spin precession damping were not been taken into account. The effective one-dimensional spin conductivity of a normal metal layer connected in series with the spin conductivity of the gext interface contributes to the effective spin conductivity of the structure [26, 27].

$$g_{eff} = (1/g^{\uparrow\downarrow} + 1/g_{ext}). \quad (3)$$

The expression for g_{ext} is obtained by solving the spin diffusion equation with the corresponding boundary conditions. In the case of the ferromagnet/normal metal structure, the following spin conductivity expression was obtained [22]

$$g_{ext} = \tanh(d_{Pt}/\lambda_d)/(2\lambda_d \rho_{Pt}), \quad (4)$$

where ρ_{Pt}, d_{Pt} and λ_d are the specific resistance, thickness and diffusion length for the Pt film, respectively. For a thickness of d_{Pt} = 10 nm, exceeding λ_d = 3 nm [22], $\tanh(d_{Pt}/\lambda_d) \approx 1$, and the contribution to the line width from the spin conductivity in the Pt film is equal at room temperature:

$$\Delta H_{ext} = (\omega/\gamma) g \cdot \mu_B \cdot h/(2\pi 4 e^2 M_s d_F \rho_{Pt} \lambda_d) \approx 6\ Oe, \quad (5)$$

where g = 2, M_s = 300 *Oe*, $d_F = 4 \cdot 10^{-6}$ cm, $\rho_{Pt} = 3 \cdot 10^{-5}$ Ω cm, $\lambda_d = 3 \cdot 10^{-7}$ cm, $h/e^2 = 2.6 \cdot 10^4$ Ω. The broadening of the FMR line due to the effective spin conductivity of the normal metal layer is equal to the contribution from the spin current. The large value of this broadening is probably caused by an error in determining the spin relaxation length λ_d. The temperature dependences of the linewidth for the *b*-LSMO manganite film and for the Pt/*b*-LSMO heterostructure are presented in **Fig. 2**. With a decrease in the temperature the ΔH_{pp} markedly increased. Increasing M_s with decreasing T may cause an increase in the linewidth (see expression (5)). But below T = 200 K, the magnetization M_s is saturated, and the width of the FMR line continues to grow.

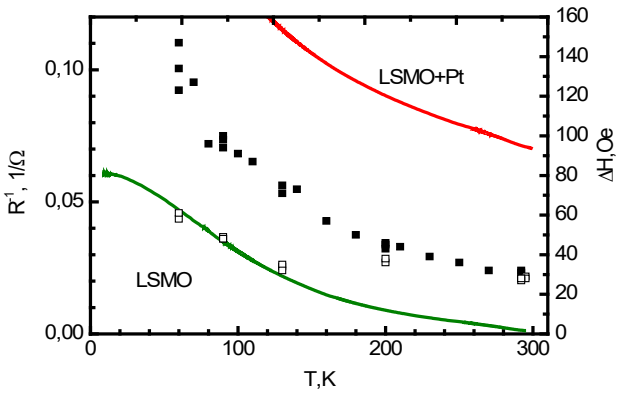

Fig. 2. *Temperature dependences of the width of the FMR lines of the b-LSMO film (open squares) and Pt/b-LSMO heterostructures (filled squares). The temperature dependences of the resistance of LSMO manganite films (green line) and Pt/b-LSMO heterostructures (red line) are presented.*

When a Pt film is deposited on top of an LSMO film, the overall conductivity of the structure increases (see Fig. 2). The increase in ΔH_{pp}, which is observed in the experiment after the deposition of Pt at low temperatures, can be fully explained by the generation of the spin current in the Pt/LSMO heterostructure. With decreasing temperature, the resistivity of the Pt film decreases in proportion to T, and the resistance of the LSMO film changes by more than one order of magnitude. The contribution of all layers to the resistivity of the heterostructure is explained by the fact that the LSMO film together with the Pt film acts as parallel resistors [28]. An increase in ΔH_{pp} with decreasing temperature can be caused by damping caused by eddy current, which is proportional to the conductivity of the structure.

3. FMR FOR TCFC/LSMO HETEROSTRUCTURE

The FMR spectrum of the TCFC/LSMO heterostructure presented in **Fig. 3**a, was measured at the frequency $\omega/2\pi$ = 9.74 GHz at T = 300 K with a constant field lying in the plane of the heterostructure and directed along the axis of easy magnetization of the heterostructure. Three areas of ferromagnetic order are visible in the structure. The temperature dependences of the resonance fields H_0 for three lines of the FMR spectrum are shown in Fig. 3b. The line in the

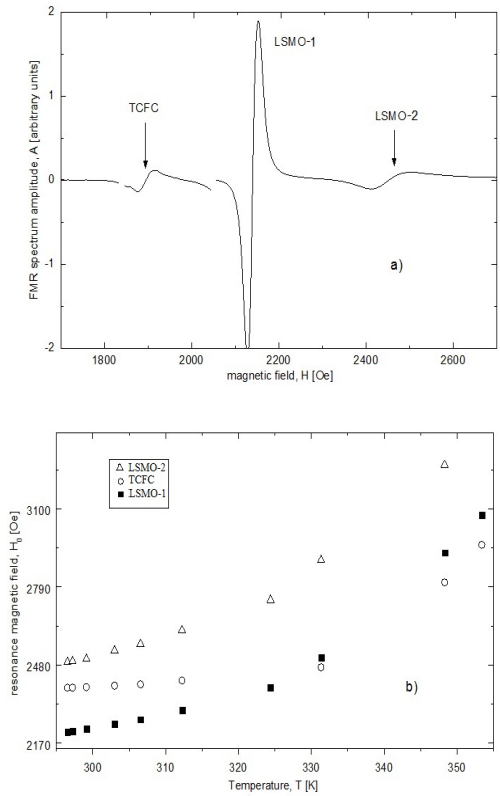

Fig. 3. *(a) FMR spectrum of the TCFC/LSMO heterostructure. The constant magnetic field is directed along the easy axis of magnetization, T = 300K. The scale of the TCFC superlattice line has been increased 10 times. (b) Temperature dependences of the resonant magnetic field for three lines of FMR. Triangles, filled rectangles and circles refer to LSMO-2, LSMO-1 and TCFC film correspondingly*

1900 Oe area in Fig. 3a is caused by the presence of a TCFC superlattice in the structure. It is seen that at $T \leq 300$ K, the field $H_0(T)$ of this line slowly decreases with decreasing temperature, which indicates a high Curie temperature of the film (above 360 K). Two other lines refer to the LSMO film: LSMO-2 corresponds to the part of the LSMO film that lies under the TCFC superstructure, while LSMO-1 refers to the part of the LSMO film that is not covered by the TCFC film. The number of electron spins for the LSMO-1 and LSMO-2 peaks is determined by the topology of the sample (the area covered by the TCFC and the non-covered parts of the chip). Estimation of the number of spins was carried out by calculating the area of the absorption line of the FMR spectrum. The widths of the FMR spectra (ΔH) of these two lines of the LSMO film differ by 40–50 Oe.

Since both parts of LSMO-1 and LSMO-2 are located on the same substrate and have the same crystal structure, the observed difference of ΔH in peaks is most likely caused by the interaction of the TCFC superlattice and LSMO film. A similar broadening of the FMR line for structures with ferromagnet/normal metal interfaces was observed previously (see the part 2 of the article) and is explained theoretically [19] by the spin current leaving the ferromagnet in a normal metal during FMR.

Solving the Landau-Lifshitz-Gilbert equation gives two resonance relations $\omega(H_0)$, describing the FMR in TCFC and LSMO-2 films. With allowance for uniaxial and biaxial anisotropies, these relations are similar to those obtained in [29] for an autonomous LSMO film deposited on an (011) $NdGaO_3$ orthorhombic substrate, which causes the uniaxial magnetic anisotropy [20]. Taking into account the magnetic interaction in the expressions for the resonant frequency $\omega(H_0)$[20], the value of H_0 should be replaced by the sum of two terms $H_{01} + H_{J1}$ and $H_{02} + H_{J2}$ for the LSMO-2 film and TCFC superlattices, respectively. Here, $H_{J1} = J/(M_1 d_1)$ and $H_{J2} = J/(M_2 d_2)$ (d_1 and d_2 of the thickness of the LSMO and TCFC layers, respectively) give an effective interlayer exchange interaction for the LSMO-2 and TCFC films.

To determine the structure parameters, we first calculate the angular dependence of the FMR response of an autonomous LSMO film (LSMO-1). Then, using the magnitude of the magnetization obtained by fitting the dependence of the resonant field on the angle, we calculate the angular dependence of H_0 for the LSMO-2 film. Then, the exchange interaction constant J is determined. Finally, the obtained value J is used to calculate the angular dependence of H_0 for the TCFC film and for calculating the value M_2. As a result, the data obtained allow us to conclude that the TCFC/LSMO interface can be characterized by antiferromagnetic interlayer interaction with a constant J = -0.24 erg/cm.

4. RARE-EARTH INTERMETALLIC SUPERLATTICES

The structure in the form of a 'sandwich' (FeCo/$TbCo_2$/FeCo)/MgO/(FeCo/$TbCo_2$/FeCo) (TCFCM), which is promising for creating the magnetically controlled switches, was investigated [30]. The two films (in brackets) are three-layer polycrystalline films of intermetallic compounds with a thickness of 2 nm (FeCo) and 6 nm ($TbCo_2$), which are separated by a thin layer of MgO with a thickness of 3 nm. This structure was deposited on a silicon substrate with dimensions of 5×5×0.5 mm^3. Both intermetallic films are ferromagnets at room temperature with giant magnetostriction. During deposition of intermetallic films the external magnetic field was applied in parallel to the substrate plane, keeping the same direction, but with significantly different intensities for each of compounds. In this case, it was expected that the easy axis $\mathbf{n}_u$ magnetic anisotropy of the films will lie in their plane and will be oriented along the imposed magnetic field, while their magnetic anisotropy constants will be significantly different.

Recently, ferromagnetic films with in-plane uniaxial anisotropy of the magnetic field revealed the effect of a sharp increase in the radio frequency (RF) dynamic magnetic susceptibility [23, 31–33]. It is observed when the external magnetic field H_0 lies in the film plane and directed perpendicular to its easy magnetization axis $\mathbf{n}_u$ (and, therefore, parallel relative to the hard axis direction) and passes through the value $H_0 = H_u$, where H_u is the field of uniaxial intra-planar magnetic anisotropy of the film. In this case, the recording radio frequency magnetic field $he^{i\omega t}$ is directed perpendicular to the field H_0, and its frequency ω is fixed. The effect manifests itself in the form of a relatively narrow resonance-like absorption signal with a maximum at $H_0 = H_u$. A feature of this signal is that when another frequency ω is set being changed over wide limits, the field at which it is observed remains unchanged and is equal to $H_0 = H_u$. This effect, called the "magnetic pseudo-resonance" [23], is caused by the loss of stability of the magnetic system at the critical point $H_0 = H_u$ of the transition from the angular phase to the collinear one with a direction of magnetization parallel to the external field [33].

To search for a pseudo-resonance signal, the TCFC film structure was placed in a Q-meter sensor coil. The signal was recorded by the method of synchronous detection with a bi-directional sweep of the H_0 field, additionally modulated with the frequency of 52.3 kHz and the amplitude of 1.3 Oe. Signal registration was carried out continuously with multiple accumulations (up to 100 times). The received signal is shown in **Fig. 4**. Two components are clearly seen, corresponding to the two pseudo-resonance signals. We note that the shape of these signals differs markedly from the derivative of absorption in a magnetic field that is usual for EPR spectroscopy. The distortions are due to the high sensitivity of the pseudo-resonance signals to the orientation of the modulating field, which in our experimental conditions has a small transverse component. Without dwelling on the details, we confine ourselves to stating the fact that the two observed components of the RF absorption spectrum correspond to two pseudo-resonance

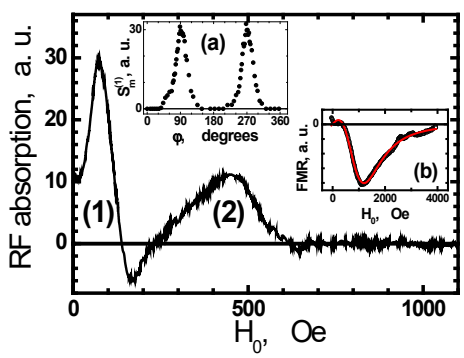

Fig. 4. *Radio-frequency absorption in a ferromagnetic heterostructure film (FeCo/$TbCo_2$/FeCo)/MgO/(FeCo/$TbCo_2$/FeCo) consisting of two three-layer films (in brackets), separated by a layer of MgO, depending on the external magnetic field H_0, oriented perpendicular to the nu axis of the easy magnetization.*

signals, 1 and 2, with maxima at H_0* around 74 Oe and 456 Oe, respectively. Different values of H_0* for these signals mean that the magnetic anisotropy fields H_u in sandwich-type films are significantly different. For signal 1, the dependence $S_m^{(1)}(\varphi)$ of its maximum on angle φ was removed (inset (a) in Fig. 4). It was obtained by scanning the field H_0 in a relatively narrow range of 0–140 Oe at angles φ, including the values φ = 90° and 270°. It can be seen that in both cases the dependencies are almost the same. They turn out to be much smoother than a similar dependence for the LSMO film: their width at half-height reaches 40°. As a result, the average direction of the axis of difficult magnetization for film 1 corresponds to the angle φ = 90° with an accuracy of ±4°. Similar measurements for film 2 with a wider pseudo-resonance line yielded the value φ = 90° ± 12°. From this it follows that in both films of the TCFCM structure the directions of the axes of the intra-plane magnetic anisotropy almost coincide.

It is natural to compare the data obtained for the described heterostructure with what gives FMR at a frequency of 9.78 GHz. Inset (b) is Fig. 4 shows the FMR signal from this structure, which is a derivative of the FMR absorption signal. It was obtained by the method of synchronous detection when sweeping the H_0 field under conditions of its modulation with a frequency of 100 kHz and amplitude of 10 Oe and using 4-fold accumulation. It can be seen that the signal is very broad, there is no resolved structure in it, corresponding to two films with significantly different values of the anisotropy field H_u. Experimentally, it was not possible to identify it for all possible orientations of the sample in the H_0 field. It also could not be detected by modeling the signal with the sum of two lines with the shape characteristic of FMR under the conditions of our experiment. At the same time, it is well described by a single Lorentzian with a width at half-height $\Delta_{1/2}$ = 1024 ± 6 Oe and a resonant field H_0 = 675 ± 2 Oe (the solid curve in inset b in Fig. 4). The unusual sharply asymmetric form of this spectrum is explained by the fact that resonance is observed in low fields ($H_0 \sim \Delta_{1/2}$), when both rotational components of the high-frequency field are effective [34].

Returning to the pseudo-resonance spectrum (Fig. 4), we emphasize once again that it consists of two well-resolved signals corresponding to different values of the field H_u in the films. In addition, from the signals in the inset (a) to Fig. 4, the direction of the n_u axis is also determined, which in this case cannot be done with the help of the FMR spectrum. This suggests that magnetic pseudo-resonance recorded at a frequency of hundreds of MHz may be a useful addition to the ferromagnetic resonance in the microwave range in the study of thin ferromagnetic films with uniaxial planar magnetic anisotropy. Note that the above values of the field H_0*, corresponding to the maxima of the signals of pseudo-resonance 1 and 2, cannot be identified with the values of the fields H_u in isolated ferromagnetic films. In complex structures such as TCFCM, interlayer exchange interactions usually occur, which can lead to renormalization of the anisotropy fields and the corresponding shift of the maximum of the pseudo-resonance in a magnetic field.

5. SPIN CURRENT IN TCFC/$Y_3Fe_5O_{12}$ STRUCTURE

Films from $Y_3Fe_5O_{12}$ (YIG) are very attractive for spintronic structures because of the small magnetic attenuation and the fact that they are an insulator. It was reported that the spin current can be excited in YIG and detected with a Py film [3-5]. **Fig. 5** presents the results of experimental studies of the inverse spin-Hall effect (ISHE) in the TCFC/YIG heterostructure. The YIG epitaxial film with a thickness of 5 μm was grown on a (111) $Gd_3Ga_5O_{12}$ (GGG) substrate. The [$TbCo_2$(5nm)/Cu(0.4nm)/

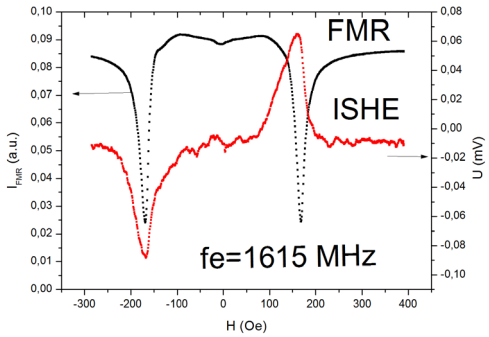

Fig. 5. *The FMR spectrum of an epitaxial YIG film grown on a GGG substrate, on top of which* $[TbCo_2(5nm)/Cu(0.4nm)/FeCo(5nm)/Cu(0.4nm)]_3$ *superlattices were deposited, 32 nm thick. The reverse spin-Hall effect signal appearing from the superlattice is shown by the red line.*

$FeCo(5nm)/Cu(0.4nm)]_3$ ($TCFC_C$) 32 nm thick superlattice was deposited. On the surface of the heterostructure, contact pads were formed to measure the potential difference caused by the ISHE effect. The sample was placed on a strip microwave line located in the gap of the electromagnet, with which FMR was excited in the YIG film. When the magnetizing field was changed, the potential difference ISHE and the intensity of the FMR signal were recorded. Fig. 5 shows the FMR spectrum of a YIG film, taken in a microstrip configuration at a frequency of 1615 MHz at T = 300 K, a generator power of 2 mW and a magnetic field that lies in the plane of the substrate and directed along the hard axis of magnetization. At H = 169 ± 0.2 Oe, a peak is observed, caused by FMR in the YIG film. There is a slight asymmetry of the peak position relative to a change in the polarity of the magnetic field. The peak half-width is 24 Oe. The second peak caused by ferromagnetism of TCFC is not observed due to the small thickness of the layer.

Fig. 5 also shows the dependence of the voltage of the inverse spin-Hall effect measured on the $TCFC_C$ film on the magnetic field. A strong asymmetry of the ISHE peak of ~ 7 Oe is observed. The ISHE peak width was 60 Oe. When the direction of the magnetizing field was changed, a change in the ISHE sign of voltage was observed, the value of which reached 80 μV.

The implementation of ISHE in ferromagnetic metals significantly expands the types of materials that could be used to study the spin current, including the rare-earth materials of the lanthanum group with extremely large spin-Hall angles, such as manganites, ruthenates, and etc.

6. CONCLUSION

Experimental studies of the magnetic properties of heterostructures consisting of epitaxially grown manganite LSMO and rare-earth intermetallic superlattices consisting of exchange-coupled TCFC layers showed that the magnetic interaction in the heterostructure has an antiferromagnetic character. After the deposition of a thin Pt film on top of the LSMO manganite film, an increase in the ferromagnetic resonance line width was observed due to the spin current flowing in Pt, which occurs in the LSMO film at resonance. An electric voltage caused by the inverse spin Hall effect in a TCFC film was experimentally observed under conditions of ferromagnetic resonance in an yttrium iron garnet.

ACKNOWLEDGMENTS

This work was partially supported by the RFBR project 18-57-16001 in the framework of the international laboratory LEMAC-LICS. The authors are grateful to A.E. Mefyod and I.V. Borisenko for help with the work and useful discussions.

REFERENCES

1. Dyakonov MI, Perel VI. Current-induced spin orientation of electrons in semiconductors. *Phys. Lett. A*, 1971, 35:459.
2. Saitoh E, Ueda M, Miyajima H, and Tatara G. Conversion of spin current into charge current at room temperature: Inverse spin-Hall effect. *Appl. Phys. Lett.*, 2006, 88:182509.
3. Miao BF, Huang SY, Qu D, Chien CL. Inverse Spin Hall Effect in a Ferromagnetic Metal. *Phys. Rev. Lett.*, 2013, 111:066602.
4. Hyde P, Lihui Bai, Kumar DMJ, Southern BW, Hu C-M, Huang SY, Miao BF, Chien CL. Electrical detection of direct and alternating

spin current injected from a ferromagnetic insulator into a ferromagnetic metal. *Phys. Rev. B,* 2014, 89:180404(R).
5. Yang F, Hammel PC. FMR-driven spin pumping in $Y_3Fe_5O_{12}$-based Structures. *J. Phys. D: Appl. Phys*., 2018, 51:253001.
6. Gall Y, Ben J, Socha F, Tiercelin N, Preobrazhensky V, Pernod P. Low field anisotropic magnetostriction of single domain exchange-coupled (TbFe/Fe) multilayers. *J. Appl. Phys*, 2000, 87:5783.
7. Quandt E, Ludwig A, Lord DG, Faunce CA. Giant magnetostrictive thin films for applications in microelectromechanical systems. *J. Appl. Phys*., 1998, 83:7267.
8. Haghiri-Cosnet AM, Renard JP. CMR manganites: physics, thin films and devices. *J. Phys. D: Appl. Phys*., 2003, 36:R127.
9. Luo GY, Chang CR, Lin JG. Influence of damping constant on inverse spin hall voltage of $La_{0.7}Sr_{0.3}MnO_3$(x)/platinum bilayers. *J. Appl. Phys*., 2014, 17C508:115.
10. Atsarkin VA, Sorokin BV, Borisenko IV, Demidov VV, Ovsyannikov GA. Resonance spin–charge phenomena and mechanism of magnetoresistance anisotropy in manganite/metal bilayer structures. *J. Appl. Phys. D*, 2016, 49:125003.
11. Vonsovskii SV. *Ferromagnetic resonance; the phenomenon of resonant absorption of a high-frequency magnetic field in ferromagnetic substances.* Ferromagnetic Resonance Academic, New York, 1966.
12. Verhagen TGA, Tinkey HN, Overweg HC, van Son M, Huber M, van Ruitenbeek JM, Aarts J. Temperature dependence of spin pumping and Gilbert damping in thin Co/Pt bilayers. *J.Phys. Condens. Matter*., 2016, 28:056004.
13. Platow W, Anisimov AN, Dunifer GL, Farle M, Baberschke K. Correlations between ferromagnetic-resonance linewidths and sample quality in the study of metallic ultrathin films. *Phys Rev. B*, 1998, 58:5611.
14. Flovik V, Macia F, Kent AD, Wahlstrom E. Eddy current interactions in a ferromagnet-normal metal bilayer structure, and its impact on ferromagnetic resonance lineshapes. *J. Appl. Phys*., 2015, 117:143902.
15. Flores AG, Zazo M, Raposo V, Iniguez J. Ferromagnetic resonance and electric characterization in double perovskite Sr_2FeMoO_6. *J. Appl. Phys*., 2003, 93:8068.
16. Heinrich B, Urban R, Woltersdorf G. Magnetic relaxation in metallic films: Single and multilayer structures. *J. Appl. Phys*., 2002, 91:7523.
17. Heinrich B, Woltersdorf G, Urban R. Role of dynamic exchange coupling in magnetic relaxations of metallic multilayer films (invited). *J. Appl. Phys.*, 2003, 93:7545-7550.
18. Beaujour J-M, Ravelosona D, Tudosa I, Fullerton EE, Kent AD. Ferromagnetic resonance linewidth in ultrathin films with perpendicular magnetic anisotropy. *Phys. Rev. B*, 2009, 80:180415(R).
19. Tserkovnyak Ya, Brataas A, Bauer GEW. Enhanced Gilbert damping in thin ferromagnetic films. *Phys.Rev.Lett*, 2002, 88:117601.
20. Ovsyannikov GA, Petrzhik AM, Borisenko IV, Klimov AA, Ignatov YuA, Demidov VV, Nikitov SA. Magnetoransport Characteristics of Strained $La_{0.7}Sr_{0.3}MnO_3$ Epitaxial Manganite Films, *JETP*, 2009, 135:56.
21. Luo GY, Belmeguenai M, Roussigne Y, Chang CR, Lin JG, Cherif SM. Enhanced magnetic damping in $La_{0.7}Sr_{0.3}MnO_3$ capped by normal metal layer. *AIP Adv.*, 2015, 5:097148.
22. Rojas-Sanchez J-C, Reyren N, Laczkowski P, Savero W, Attane J-P, Deranlot C, Jamet M, George J-M, Vila L, Jaffr`es H. Spin pumping and inverse spin Hall effect in platinum: the essential role of spin-memory loss at metallic interfaces. *Phys. Rev. Lett.*, 2014, 112:106602.
23. Atsarkin VA, Demidov VV, Mefed AE, Nagorkin VYu. Magnetic Pseudoresonance in Manganite Thin Films. *Appl. Magn. Reson*., 2014, 45:809.

24. Mosendz O, Vlaminck V, Pearson JE, Fradin FY, Bauer GEW, Bader SD, Hoffmann A. Detection and quantification of inverse spin Hall effect from spin pumping in permalloy/normal metal bilayers. *Phys. Rev. B,* 2010, 82:214403.
25. Rezende TM, Rodrıguez-Suarez RL, Soares MM, Vilela-Le LH, Domınguez DL, Azeved A. Enhanced spin pumping damping in yttrium iron garnet/Pt bilayers. *Appl. Phys. Lett.*, 2013, 102:012402.
26. Emori S, Alaan US, Gray MT, Sluka V, Chen Y, Kent AD, Suzuki Y. Spin transport and dynamics in all-oxide perovskite $La_{2/3}Sr_{1/3}MnO_3/SrRuO_3$ bilayers probed by ferromagnetic resonance. *Phys. Rev. B.*, 2016, 94:224423.
27. Boone CT, Nembach HT, Shaw JM, Silva TJ. Spin transport parameters in metallic multilayers determined by ferromagnetic resonance measurements of spin-pumping. *J. Appl. Phys.,* 2013, 113:153906.
28. Boone CT, Shaw JM, Nembach HT, Silva TJ. Spin-scattering rates in metallic thin films measured by ferromagnetic resonance damping enhanced by spin-pumping. *J. Appl. Phys.*, 2015, 117:223910.
29. Demidov VV, Ovsyannikov GA, Petrzhik AM, Borisenko IV, Shadrin AV, Gunnarsson R. Magnetic anisotropy in strained manganite films and bicrystal junctions. *J. Appl. Phys.*, 2013, 113:163909.
30. Borisenko IV, Demidov VV, Klimov AA, Ovsyannikov G.A, Konstantinyan K.I, Nikitov SA, Preobrazhenskii VL, Tiercelin N, and Pernod P. Magnetic Interaction in the Manganite/Intermetallic Compound Heterostructure. *Technical Physics Letters,* 2016, 42:113.
31. Belyaev BA, Izotov AV, Kiparisov SYa. The peculiarity of the high-frequency susceptibility of thin magnetic films with uniaxial anisotropy. *JETP Lett,* 2001, 74(4):226-230.
32. Vasilevskaya TM, Sementsov DI. Ferromagnetic resonance in a uniaxial magnetic film with bias along the axis of a difficult magnetization. JETP, 2010, 110(5):754.
33. Klimov A, Ignatov Yu, Tiercelin N, Preobrazhensky V, Pernod P, Nikitov S. Ferromagnetic resonance and magnetoelasticde modulation in thin active films with anuniaxial anisotropy. *J. Appl. Phys.*, 2010, 107:093916.
34. Altshuller SA, Kozyrev BM. *Electron Paramagnetic Resonance in Compounds of Intermediate Group Elements.* Moscow, Nauka Publ., 1972.